DOI: 10.1002/adsc.201000606

Acid-Free Nickel Catalyst for Stereo- and Regioselective Hydrophosphorylation of Alkynes: Synthetic Procedure and Combined Experimental and Theoretical Mechanistic Study

Valentine P. Ananikov,[a,*] Levon L. Khemchyan,[a] Irina P. Beletskaya,[b,*] and Zoya A. Starikova[c]

[a] Zelinsky Institute of Organic Chemistry, Russian Academy of Sciences, Leninsky Prospect 47, Moscow 119991, Russia
Fax: (+7)-499-135-5328; e-mail: val@ioc.ac.ru
[b] Lomonosov Moscow State University, Chemistry Department, Vorob′evy gory, Moscow 119899, Russia
Fax: (+7)-495-939-3618; e-mail: beletska@org.chem.msu.ru
[c] Nesmeyanov Institute of Organoelement Compounds, Russian Academy of Sciences, Vavilova str. 28, Moscow, 119991, Russia

Received: July 29, 2010; Published online: November 17, 2010

Supporting information for this article is available on the WWW under http://dx.doi.org/10.1002/adsc.201000606.

Abstract: The nickel catalyst prepared *in situ* from nickel bis(acetylacetonate) [$Ni(acac)_2$] precursor and bis(diphenylphosphino)ethane (DPPE) ligand has shown excellent performance in the hydrophosphorylation of alkynes. Markovnikov-type regioselective addition to terminal alkynes and stereoselective addition to internal alkynes were carried out with high selectivity without an acidic co-catalyst (in contrast to the palladium/acid catalytic system). Various H-phosphonates and alkynes reacted smoothly in the developed catalytic system with up to 99% yield. The mechanisms of catalyst activation and C–P bond formation were revealed by experimental (NMR, ESI-MS, X-ray) and theoretical (density functional calculations) studies. Two different pathways of the alkyne insertion in the coordination sphere of the metal are reported for the first time.

Keywords: alkynes; homogeneous catalysis; nickel complexes; phosphorylation; selectivity

Introduction

Transition metal-catalyzed addition reactions fulfill green chemistry requirements in developing sustainable synthetic procedures.[1] The addition reaction is characterized with 100% atom efficiency and maximizes the incorporation of all reactants into the products. Catalytic transformation ensures high selectivity of the synthesis and avoids the formation of by-products.

The development of catalytic systems for carrying out hydrofunctionalization of unsaturated organic compounds has experienced an outstanding growth in recent years.[2] Addition of E–H bonds to unsaturated organic molecules has unambiguously proven the remarkable potential of this approach for carbon-heteroatom (C–E) bond formation. Several excellent catalytic systems were reported to carry out hydroalkoxylation, hydrothiolation, hydroamination, and other addition reactions.[3]

The addition of P–H bonds to unsaturated species is a topic of special interest as far as the synthesized organic phosphorus derivatives are in demand as ligands in catalysis,[4] as biologically active compounds,[5,6] as useful derivatives in nucleic acid chemistry,[7] as versatile reagents in synthesis,[8] as building blocks in polymer sciences,[9] as well as several material science applications including fuel cell membranes, optical materials and flame retardants.[10,11]

The unique nature of the phosphorus atom gave rise to the studies of P(III)–H and P(V)–H addition reactions. These three- and five-valent phosphorus substrates possess rather different properties in the addition reactions with a strong dependence on the nature of the substituents.[12,13,14] Particularly, the addition reactions operate according to different mechanistic frameworks and require special catalytic systems to be designed for each combination of reagents.

Hydrophosphination of unsaturated organic molecules [addition of the P(III)–H bond] appears to

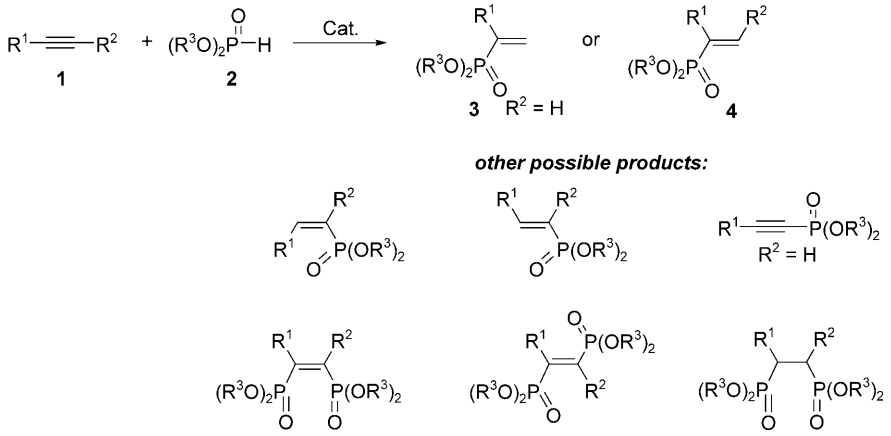

Scheme 1. Alkyne hydrophosphorylation reaction towards the formation of Markovnikov product **3** (terminal alkynes), *syn*-addition product **4** (internal alkynes) and possible by-products.[19]

be an actively developing area with several bright achievements in the mechanistic studies and synthetic applications.[13,15]

In contrast, the mechanistic nature of the addition of the P(O)–H bond is scarcely understood. The reaction is rather difficult to carry out with high selectivity since a variety of products may be formed (Scheme 1).[12] The field was pioneered by Tanaka and co-workers, who reported the catalytic Markovnikov hydrophosphorylation of alkynes by application of transition metal catalysts and described the effect of the $Ph_2P(O)OH$ acid.[16] Recently we have studied the Pd/CF_3COOH catalytic system for the selective hydrophosphorylation of alkynes using different types of H-phosphonates.[17] In these catalytic systems the addition of acid was necessary to avoid side-reactions, without the acid poor selectivity and yields of the Markovnikov product were observed.

Several disadvantages of the available catalytic systems were noticed. The acid could not be recycled (waste) and, in addition, it imposed a serious drawback for commercial implementation,[18] as well as the high cost of the palladium catalyst.

Recent advances in catalytic hydrofunctionalization encouraged us to develop a more practical catalyst beyond the Pd/acid system.

In the present study we report an acid-free catalytic system for the Markovnikov-type hydrophosphorylation of alkynes. Under optimized conditions a cheap and easily available Ni catalyst was found to be superior for this transformation. The mechanistic study revealed the unusual nature of the studied catalytic system with two possible pathways for C–P bond formation.

Results and Discussion

The performance of the catalytic reaction was evaluated using the model hydrophosphorylation reaction of 1-heptyne (**1a**) with $(i\text{-PrO})_2P(O)H$ (**2a**). The overall selectivity was calculated as the ratio between the Markovnikov product **3a** and the total amount of all other by-products.[20] Cheap and air-stable $Ni(acac)_2$ was chosen as a catalyst precursor and the reaction was carried out in THF at 100 °C (Scheme 2).

Several phosphine ligands with different electronic and steric properties did not lead to the formation of product **3a** (Entry 1, Table 1). Quantitative recovery of starting material **2a** indicated that no reaction took place under the studied conditions. Neither did most of the studied chelate bidentate ligands result in the

Table 1. Ligand effect in the Ni-mediated addition of $(i\text{-PrO})_2P(O)H$ (**2a**) to 1-heptyne (**1a**).[a]

Entry	Ligand[b]	Yield of **3a** [%][c]	Unreacted **2a** [%][c]	By-products [%][c,d]
1	PPh_3, $P(o\text{-}MeC_6H_4)_3$, PPh_2Me, PMe_2Ph, PCy_3, $P(t\text{-}Bu)_2Me$, $P(O\text{-}i\text{-}Pr)_3$	0	100	0
2	DPPM, DPPB, BINAP, DCPM	0	100	0
3	DPPE	14	84	2

[a] 1 mmol of **1a**, 1 mmol of **2a**, 3 mol% of $Ni(acac)_2$, 12 mol% of ligand (6 mol% of bidentate ligand), 0.5 mL of THF, 100 °C, 3 h.
[b] DPPM: bis(diphenylphosphino)methane; DPPB: 1,4-bis(diphenylphosphino)butane; BINAP: 2,2′-bis(diphenylphosphino)-1,1′-binaphthyl; DCPM: bis(dicyclohexylphosphino)methane; DPPE: 1,2-bis(diphenylphosphino)ethane.
[c] Determined by ^{31}P NMR.
[d] Overall amount of phosphorus-containing by-products.

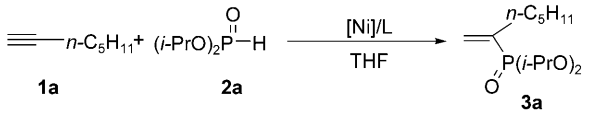

Scheme 2. Model P(O)–H bond addition reaction.

formation of **3a** (entry 2, Table 1). Surprisingly, a 14% yield of Markovnikov product **3a** was observed with DPPE. The starting material was recovered with 84% yield and only 2% of by-products were formed.

Optimization studies of the reaction conditions with the $Ni(acac)_2$/DPPE catalytic system have shown that a 53% product yield may be achieved with 6 mol% of the catalyst at 100 °C for 6 h. The reaction was highly selective, the overall amount of by-products was as small as 3%.

Stimulated with the exciting results with this $Ni(acac)_2$ system we have studied other nickel precursors in the catalytic system with the DPPE ligand (Table 2). The formation of product **3a** was not observed with $NiCl_2$ and $Ni(ClO_4)_2$, while conversion of the substrates to by-products was found, 30% and 43%, respectively (entries 1 and 2; Table 2). A minor amount of **3a** was detected in the reaction with $Ni(OAc)_2$ catalyst precursor, together with 18% of by-products (entry 3, Table 2). The $Ni(acac)_2$ and zerovalent $Ni(COD)_2$ have shown a similar performance with 52–53% product yields (entries 4 and 5; Table 2) and trace amounts of by-products (~3%).

Two important points concerning the study of catalyst precursors deserve particular notes. First, the reaction was extremely sensitive to the nature of the Ni(II) source – a dramatic difference in the yield and selectivity was observed between rather similar nickel salts. Second, $Ni(acac)_2$ was confirmed as an excellent replacement for the air-sensitive and difficult to prepare zerovalent $Ni(COD)_2$ complex.

The further optimization of reaction conditions with $Ni(acac)_2$ has shown that the yield can be increased at longer reaction times – 62% in 24 h (entry 1, Table 3), compared to 53% in 6 h (entry 4, Table 2). At this point we have analyzed the influence of various additives on the performance of the catalytic system (Table 3).

Table 2. Different metal precursors in the [Ni]/DPPE-catalyzed addition of $(i\text{-PrO})_2P(O)H$ (**2a**) to 1-heptyne (**1**).[a]

Entry	Catalyst	Yield of **3a** [%][b]	Unreacted **2a** [%][b]	By-products [%][b,c]
1	$NiCl_2$	0	70	30
2	$Ni(ClO_4)_2$	0	57	43
3	$Ni(OAc)_2$	10	72	18
4	$Ni(acac)_2$	53	44	3
5	$Ni(COD)_2$	52	45	3

[a] 1 mmol of **1a**, 1 mmol of **2a**, 6 mol% of catalyst precursor, Ni:DPPE = 1:2 (except 1:1 ratio for entry 5), 0.5 mL of THF, 100 °C, 6 h.
[b] Determined by ^{31}P NMR.
[c] Overall amount of phosphorus-containing by-products.

Table 3. Additive effects in the $Ni(acac)_2$/DPPE-catalyzed addition of $(i\text{-PrO})_2P(O)H$ (**2a**) to 1-heptyne (**1a**).[a]

Entry	Additive	Yield of **3a** [%][b]	Unreacted **2a** [%][b]	Other products [%][b,c]
1	none	62	33	5
2	$Ph_2P(O)OH$[d]	36	57	7
3	CF_3COOH[d]	0	100	0
4	Et_3N[d]	48	47	5
5	γ-terpinene[e]	61	34	5

[a] 1 mmol of **1a**, 1 mmol of **2a**, 6 mol% of $Ni(acac)_2$, 12 mol% of DPPE, 0.5 mL of THF, 100 °C, 24 h.
[b] Determined by ^{31}P NMR.
[c] Overall amount of phosphorus-containing by-products.
[d] 10 mol% of the additive.
[e] 20 mol% of the radical trap[21] additive.

Addition of acids did not improve the performance of the catalytic reaction. Moreover, the yield was decreased to 36% with $Ph_2P(O)OH$ and the reaction was suppressed with CF_3COOH (entries 2 and 3; Table 3). The result is in sharp contrast with previously reported catalytic systems, where these acids were necessary to increase the yield and selectivity of product **3** formation.[16c,17] Addition of base demonstrated a negative effect on the studied hydrophosphorylation reaction (entry 4, Table 3). A radical trap (γ-terpinene) did not influence the outcome of the addition reaction, indicating the absence of radical pathways in the studied system (entry 5, Table 3).

With the optimized parameters of the catalytic reaction in hands we have designed the synthetic procedure for the selective hydrophosphorylation of alkynes. The cheap and easily available catalyst precursor – $Ni(acac)_2$ – allowed the use of 9 mol% of the catalyst and increased the yield of product **3**. For the terminal alkynes it was important to carry out slow addition to the reaction mixture to minimize the side-reaction of triple bond polymerization.[22] The scope of designed synthetic procedure was evaluated with different H-phosphonates and alkynes (Table 4).

Terminal alkynes **1a**–**1c** smoothly reacted with **2a** at 100 °C and resulted in product formation in good yields of 61–89% (entries 1–3, Table 4). The reaction proceeded with high regioselectivity. The more challenging reaction with internal alkynes required higher temperatures of 120–140 °C to account for the slower reactivity of the alkynes. However, even at this high temperature high product yields of 80–99% and excellent *E/Z* stereoselectivity of >99/1 were observed (entries 4 and 5; Table 4).[23]

Table 4. The scope of the Ni-catalyzed $(R^3O)_2P(O)H$ (**2**) addition to alkynes **1**.[a]

Entry	Alkyne		$(R^3O)_2P(O)H$		Product	Yield [%][b]
1	**1a**	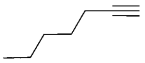	**2a**	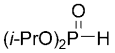	**3a**	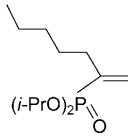	70 (63)
2	**1b**	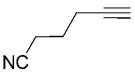	**2a**	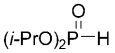	**3b**	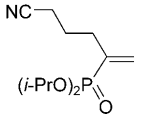	61 (53)
3	**1c**		**2a**	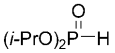	**3c**	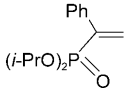	89 (81)
4	**1d**		**2a**	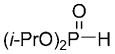	**4a**	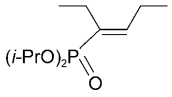	80 (69)
5	**1e**		**2a**	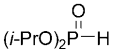	**4b**	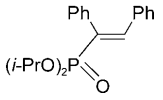	99 (94)
6	**1e**		**2b**	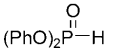	**4c**	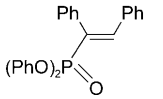	99 (89)
7	**1e**		**2c**	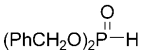	**4d**	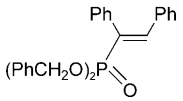	99 (96)
8	**1e**		**2d**	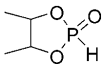	**4e**	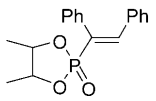	99 (98)
9	**1e**		**2e**	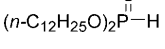	**4f**	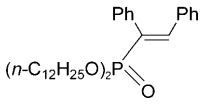	99 (98)

[a] See Experimental Section for details and conditions.
[b] Determined by ^{31}P NMR and isolated yield (in parenthesis); overall amount of impurities in all cases $<10\%$.

The developed catalytic system was tolerant to the nature of the H-phosphonates $(R^3O)_2P(O)H$. Substituents with different electronic and steric effects $R^3 = i$P-r, Ph, benzyl (entries 5–7), a cyclic H-phosphonate (entry 8) and the large n-$C_{12}H_{25}$ group (entry 9, Table 4) reacted in excellent 99% yield and $>99/1$ *E/Z* selectivity. Worthy of mention again is that a quantitative yield of the branched Markovnikov-type product (**3**) was achieved without any acidic co-catalyst.

After observing this fascinating synthetic application, we were interested to unravel the key steps of the catalytic reaction mechanism. First, we have addressed the question on the role of catalyst precursor and the dramatic differences between the nickel salts (Table 2). Chemical transformations involving all studied NiX_2 precursors (X = Cl, ClO_4, OAc, acac, COD) were investigated by ^1H and ^{31}P NMR spectroscopy, and electrospray ionization-mass spectrometry (ESI-MS).

The catalyst precursor activation step was studied in THF-d_8 solution containing NiX_2, DPPE and $(i\text{-PrO})_2P(O)H$ **2a** (Table 5). In the case of $NiCl_2$ a yellow solution was obtained with a brown insoluble precipitate (Entry 1, Table 5). The signals belonging to **2a** and DPPE remained in the THF-d_8 solution as resolved by ^1H and ^{31}P NMR. The precipitate was isolated and ESI-MS characterization showed the formation of the $[NiCl_2(DPPE)]$ complex (observed peak M−Cl = 491.0385 Da, calculated: 491.0390 Da). Dissolution of the precipitate in chloroform-d_1 showed a single resonance at $\delta(^{31}P) = 57.7$ ppm, which agrees with the literature data for this complex.

A similar procedure was carried out for the $Ni(ClO_4)_2$ precursor and showed only the signals of **2a** in the THF-d_8 solution (entry 2, Table 5). Combined ESI-MS and NMR characterization indicated formation of a mixture of the complexes $[Ni(ClO_4)_2(DPPE)]$ and $[Ni(ClO_4)_2(DPPE)_2]$.[24]

Table 5. Chemical transformations on the catalyst activation step with different nickel precursors.[a]

Entry	Catalyst	Reaction mixture	Compounds in solution[b]	Precipitate structure[b]
1	$NiCl_2$	Yellow solution and brown precipitate	**2a**, DPPE	$[NiCl_2(DPPE)]$
2	$Ni(ClO_4)_2$	Light yellow solution and yellow precipitate	**2a**	$[Ni(ClO_4)_2(DPPE)]$, $[Ni(ClO_4)_2(DPPE)_2]$
3	$Ni(OAc)_2$	Light brown solution and green precipitate	**2a**, DPPE	Unreacted $Ni(OAc)_2$
4	$Ni(acac)_2$	Dark brown solution and white precipitate	**2a**,[c], Ni/**2a** complex	DPPE dioxide
5	$Ni(COD)_2$	Dark brown solution	**2a**,[c], Ni/**2a** complex	–

[a] *Conditions:* THF-d_8, metal salt, DPPE (Ni:DPPE = 1:2) and $(i\text{-PrO})_2P(O)H$ (**2a**); for $Ni(COD)_2$ the ratio Ni:DPPE = 1:1 was used.
[b] Determined with ^1H and ^{31}P NMR, and ESI-MS.
[c] Broad signal in ^{31}P NMR.

With the $Ni(OAc)_2$ salt both **2a** and DPPE remained in the THF-d_8 solution, as well as most of the unreacted nickel acetate as a green precipitate (entry 3, Table 5). The light-brown color of the solution indicated that some trace amounts of the nickel complexes were dissolved, although it was not possible to detect them by NMR.

In the case of $Ni(acac)_2$ the salt was completely dissolved, accompanied with formation of a white precipitate (entry 4, Table 5). In the THF-d_8 a broad signal corresponding to **2a**, i.e., a broad signal at $\delta(^{31}P) = 31.5$ ppm and the signal of the dioxide of DPPE were detected. The white precipitate formed was characterized as the dioxide of DPPE, which is only partially soluble in tetrahydrofuran.

Using $Ni(COD)_2$ as a metal source the same broad signal at $\delta(^{31}P) = 31.5$ ppm as well as the broad signal of **2a** were observed.[25] The solutions obtained with $Ni(acac)_2$ and $Ni(COD)_2$ possessed identical dark brown colors.

The experiments have clearly highlighted the nature of the transformation on the catalyst activation step from the NiX_2 precursors. Stable insoluble complexes of Ni(II) with DPPE ligand were formed with X = Cl and ClO_4. The nickel complexes were not involved in the reaction of interest, thus, showing no product formation (entries 1 and 2; Table 2).[26] Trace amounts of the nickel species were in solution for the X = OAc precursor and showed a small yield in the catalytic reaction (entry 3, Table 2). Complete dissolution of the $Ni(acac)_2$ and $Ni(COD)_2$ and formation of a homogeneous catalytic system are in excellent agreement with the performance demonstrated in the addition reaction (entries 4 and 5; Table 2).

The formation of the dioxide of DPPE is important, since it indicated *in situ* reduction of the Ni(II) salt to zero-valent nickel species. Such an *in situ* reduction of divalent metal salts by phosphines is well-known in the case of palladium complexes and it was shown to produce phosphine oxides.[27] For the Ni(II) species such an *in situ* reduction by phosphines and further involvement in the catalytic cycle has scarcely been studied. The present study provides evidence for the possibility of such a generation of catalytically active nickel species from $Ni(acac)_2$.

Thus, at the first stage the reaction mechanism involved formation of zero-valent metal species *via* the reduction of divalent nickel precursor $Ni(acac)_2$ [or direct formation *via* COD replacement in $Ni(COD)_2$]. According to the generally accepted mechanistic framework, oxidative addition of the P–H bond followed by alkyne insertion (**5**) led to the formation of complex **6**, which furnished product **4** after C–H bond formation (Scheme 3). Taking into account that H-phosphonate **2** may exist in two tautomeric forms, $(RO)_2P(O)H$ and $(RO)_2POH$, the second pathway for P–H bond addition may involve alkyne coordination and external attack by the phosphorus compound (**7**).[28] Intermediate zwitterionic complexes **8a** and **8b** and nickel complex **8c** (double bond isomer of **6**) may be expected at this stage. Formation of compound **9** should be accomplished as a final product for this pathway.

It should be noted that both mechanisms – intramolecular insertion and external attack – are well known in E–H bond addition reactions catalyzed by transition metals.[2] Either of the mechanisms may take place depending on the metal, the nature of the element E and the conditions. In the case of terminal alkynes (R′ = H) it is not possible to distinguish these mechanisms based on the product structure. However, for the internal alkynes the structure of the product strongly depends on the reaction pathway: intramolecular insertion led to stereoselective formation of *syn*-addition product **4**, while external attack gave *anti*-addition product **9**.

For an unambiguous determination of the structure of the product synthesized in the studied catalytic system we have prepared single crystals of **4e** and carried out an X-ray analysis (Figure 1). The molecular

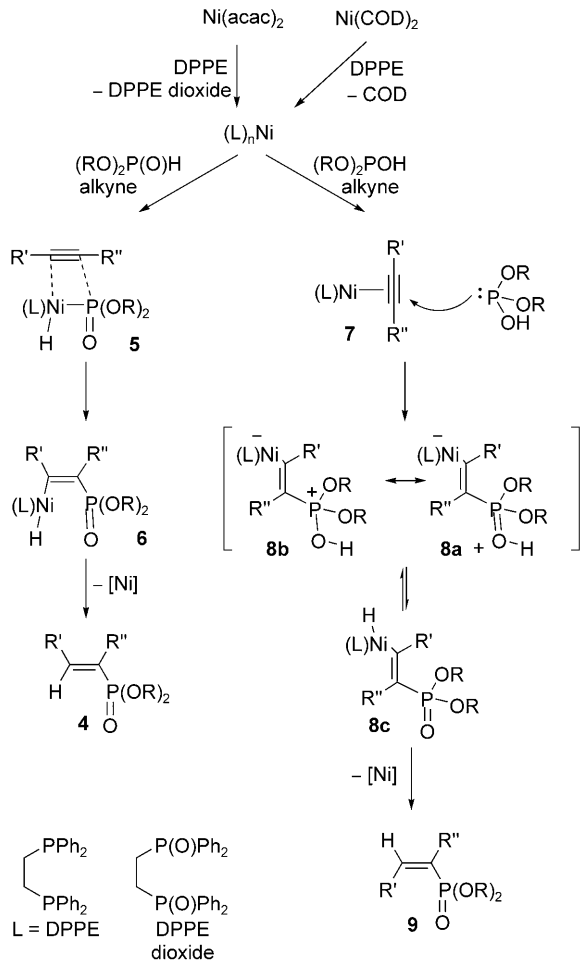

Scheme 3. Various mechanistic pathways of addition of P–H bond of H-phosphonates to alkynes.

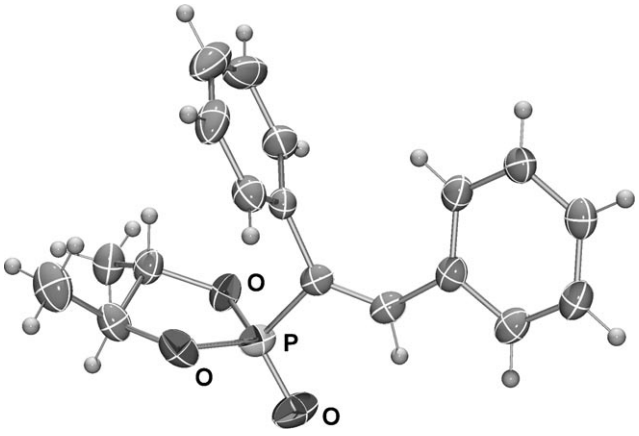

Figure 1. Molecular structure of **4e** determined by X-ray analysis.

structure of **4e** has clearly proven the *syn*-addition reaction, the hydrogen atom and phosphorus group were located in a *cis* relationship to each other. The structures of the other products **4a**–**4d** and **4f** were confirmed by measuring NMR coupling constant $^{3}J(^{31}P,^{1}H) = 20$–26 Hz, which is known to be sensitive to the geometry of the double bond. Therefore, comparing both pathways shown in Scheme 3, we may conclude that alkyne insertion is the most likely way of product formation. The high *E/Z* selectivity of the reaction $>99/1$ gave no evidence for the second pathway to make a noticeable contribution.

To reveal details of the alkyne insertion in the studied catalytic system we have performed theoretical calculations at the B3LYP/DZ(d) level.[29] The model system used in the theoretical calculations and calculated potential energy surface are shown on Figure 2, optimized geometries of intermediate complexes and transition states are given in Figure 3.[30]

Alkyne coordination to compound **I** gave a weakly bound complex and led to **II** with an energy gain of 5.2 kcal mol^{-1}. Starting from complex **II** the transition state of alkyne insertion **III-TS** was located with the calculated energy barrier of 12.2 kcal mol^{-1}. Interestingly, movement along the reaction coordinate towards formation of product **IV** facilitated dissociation of one of the phosphorus atoms of the bidentate ligand. In the product **IV** two σ-bonds, Ni–C and C–P, were formed, and the oxygen atom of the P=O group was coordinated to the metal. The reaction was highly exothermic with the energy gain of 40.1 kcal mol^{-1} compared to the initial point **I** and 34.9 kcal mol^{-1} compared to point **II**.

Tautomerization of H-phosphonates inspired us to investigate the possibility of this transformation in the metal complex **I**. Indeed, conversion of the phosphorus(V) center in **I** to a phosphorus(III) center in **VI** was feasible with a 14.9 kcal mol^{-1} activation barrier through the **V-TS**. Compound **VI** was found to be less stable than **I** by 8.7 kcal mol^{-1}. This finding was in agreement with the literature data for the free H-phosphonate, where the $(RO)_2P(O)H$ form was also found to be more stable compared to the $(RO)_2POH$ tautomer.[31]

Alkyne coordination to **VI** led to the weakly bound complex **VII** with an energy gain of 6.2 kcal mol^{-1}. To our great surprise, quantum chemical calculations of the further reaction pathway led to discovery of transition state **VIII-TS** corresponding to the reaction with alkyne. A cyclic five-membered structure was obtained and the movement along reaction coordinate involved breakage of the Ni–O bond and formation of the Ni–C and C–P bonds in product **IX**. Conversion of phosphorus(III) to phosphorus(V) took place in the phosphonate residue during this stage. The activation barrier of 23.0 kcal mol^{-1} was calculated for **VIII-TS** starting from complex **VII**. The formation of **IX** was highly exothermic with an energy gain of 37.7 kcal mol^{-1} compared to the initial point **I** and 40.2 kcal mol^{-1} compared to point **VII**.

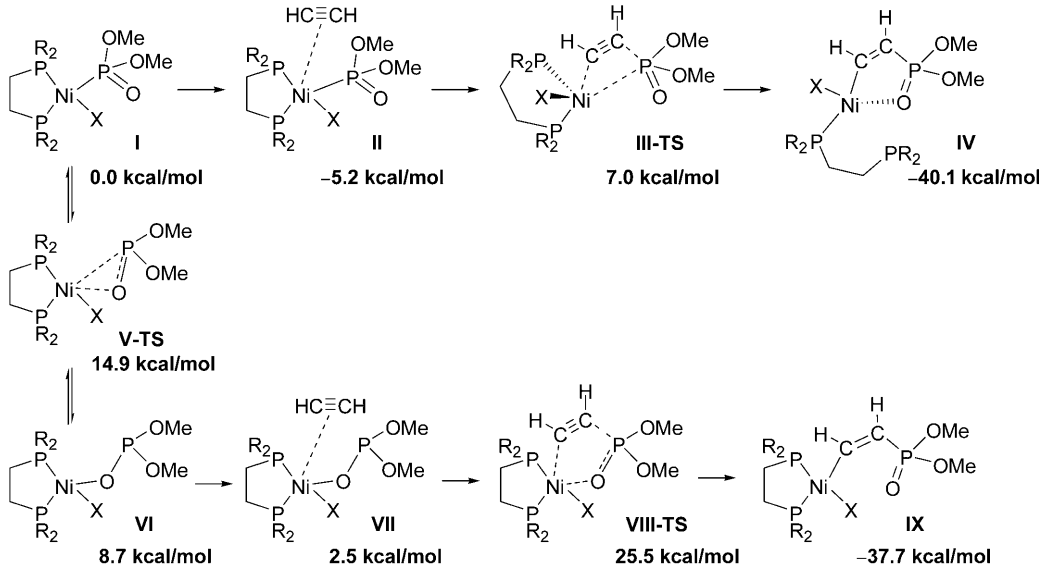

Figure 2. Calculated potential energy surface of the alkyne insertion in the nickel complexes at B3LYP/DZ(d) level (energy data for X = H is shown).

Both phosphorus atoms of the bidentate ligand remained coordinated to the nickel center during the **VI**→**IX** pathway, in contrast to the **I**→**IV** pathway, which required dissociation of one the phosphorus atoms of the ligand. If the Ni–P bonds lengths were fixed during geometry optimization of the **I**→**IV** pathway (dissociation restricted calculations), it was not possible to reach the transition state of alkyne insertion.

Here we briefly discuss the optimized molecular structures of **I**–**IX** to get a better insight into the mechanistic aspects of these transformations (structures and selected geometry parameters are provided in Figure 3). Initial complex **I** possessed the geometry typical for a square planar Ni(II) derivative with 2.23–2.24 Å length for the Ni–P_{ligand} bonds and 2.188 Å for the Ni–P1(O) bond. Approach of the alkyne towards the metal complex first led to weakly bound derivative **II**, the distances Ni–C2 = 2.351 Å and H1–O3 = 2.266 Å were found in the optimized geometry. Coordination of the alkyne in **II** only slightly effected the lengths of the Ni–P bonds. While in the π-complex **IIa** (Ni–C1 = 2.146 Å, Ni–C2 = 2.175 Å) coordination of the alkyne distorted the geometry and resulted in formation of a five-coordinated complex. Stronger binding of the alkyne activated both the C1–C2 triple bond and Ni–P1(O) bond, which became longer by 0.021 and 0.071 Å, respectively (*cf.* complexes **II** and **IIa**). The energy gain due to alkyne coordination compensated for some decrease of stability originating from the disfavored geometry. As a result of both of these effects, a similar relative stability was found for the **IIa** (−8.4 kcal mol^{-1}) and the activation energy from **IIa** to **III-TS** was calculated to be 15.4 kcal mol^{-1} (only structure **II** is shown on Figure 2 for clarity).

Starting from **IIa** the transition state **III-TS** was located corresponding to the alkyne insertion into the Ni–P1(O) bond. Movement along the reaction coordinate towards the transition state caused elongation of the of the Ni–P2 bond with complete dissociation of this metal-ligand bond in the optimized structure of product **IV** (Ni–P2 = 4.212 Å). Binding of the vinyl phosphonate ligand in the chelate fashion (Ni–C1 = 1.905 and Ni–O1 = 2.033 Å) restored the square-planar geometry of the Ni(II) complex in **IV**.

Another pathway involved isomerization of the initial nickel complex with the P(V) center to the corresponding nickel derivative containing P(III) center instead. The transformation was calculated to take place *via* the transition state **V-TS**. During this tautomerization the Ni–P1 bond was broken and a new Ni–O1 bond was formed in **VI** (Ni–O1 = 1.835 Å). The geometry arrangement of the phosphorus atom in **VI** was typical for the P(III) derivative, the P1–O1 bond was elongated from 1.501 Å (**I**) to 1.598 Å (**VI**) indicating transition from a double to a single phosphorus-oxygen bond.

Surprisingly, the very unusual transition state **VIII-TS** of the alkyne insertion was located starting directly from the complex **VII**. The unique nature of this transition state involved formation of the Ni–C1 and C2–P1 bonds *via* the five-membered structure in contrast to **III-TS**, where a four-membered transition state was adopted. The longer Ni–C1 and C2–P1 bonds were calculated for the **VIII-TS** compared to the **III-TS**.

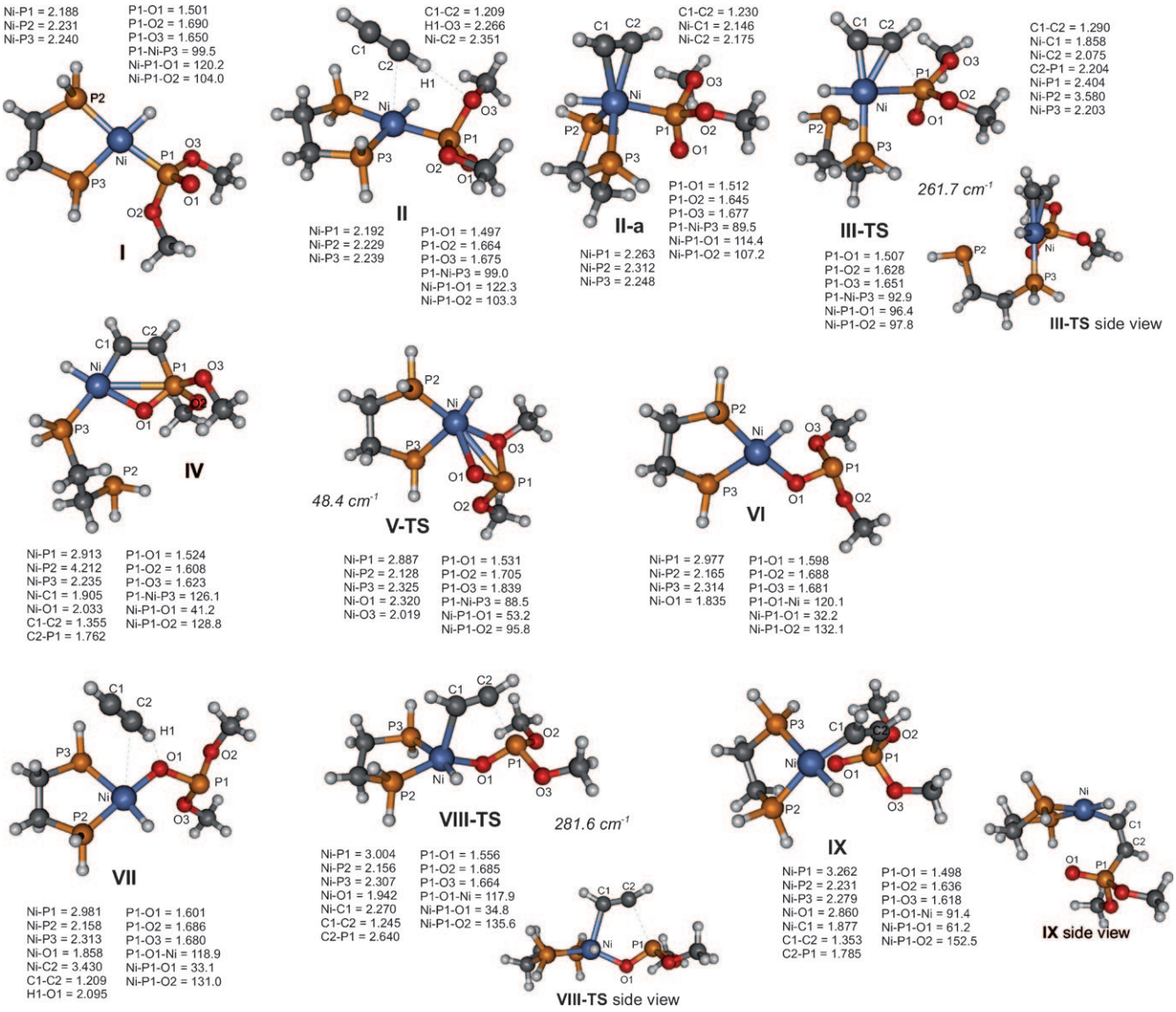

Figure 3. Optimized molecular structures of intermediate complexes and transition states at B3LYP/DZ(d) level.

Overcoming the transition state **VIII-TS** resulted in formation of two new σ-bonds, Ni–C1 and C2–P1 as well as a π-bond P1–O1, accompanied with synchronous breakage of the Ni–O1 bond and one of the acetylenic π-bonds. According to the geometry arrangement of the phosphorus atom in the product **IX** a typical P(V) center was formed (P1–O1 = 1.498 Å, P1–O2 = 1.636 Å, P1–O3 = 1.618 Å). The vinyl phosphonate ligand in **IX** was not bound in the chelate fashion like in **IV**, although some weak interaction between the Ni and O1 may take place (Ni–O1 = 2.860 Å; see side view). In both products **IX** and **IV** the same vinyl group was formed with a standard double bond length C1–C2 = 1.35 Å.

According to calculated energy surface both pathways may contribute to product formation in the studied catalytic system.[32] From an experimental point of view the pathways cannot be distinguished based on the product structure, since both operate as a *syn*-addition of the P–H bond to alkyne. Both pathways were found to be highly exothermic (Figure 2) and complexes **IV** and **IX** can be interconverted between each other through intermolecular dissociation/association of phosphorus and oxygen heteroatoms to the metal center. Thus, it would be hardly possible to distinguish the pathways with kinetic measurements. It is a valuable advantage of theoretical calculations that allowed us to unravel the mechanistic data, which was not evident from the experiment alone.

To summarize, the theoretical calculations clearly highlighted the importance of tautomerization of the metal phosphorus species and revealed a previously unknown pathway of alkyne insertion through the five-membered transition state. Another important

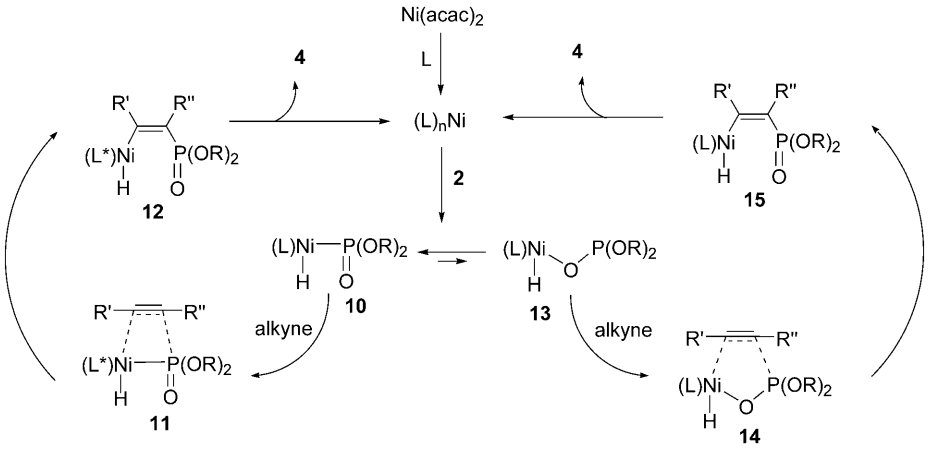

Scheme 4. Plausible catalytic cycles of the P–H bond addition to alkynes (L and L* denote different coordination types of the bidentate ligand; see Figure 2 and text for details).

point is destabilization of the well-known pathway involving **III-TS** by the strongly bound bidentate ligand.

Combining experimental and theoretical data, the following plausible catalytic cycle with $Ni(acac)_2$ as precursor may be proposed (Scheme 4).[33] Catalyst activation to form zero-valent nickel species, followed by reaction with H-phosphonate led to complexes **10** and **13** with the equilibrium shifted to the left. Starting with complex **10** the reaction mechanism includes alkyne insertion to form **11** and repeats the catalytic cycle after release of product **4** from complex **12**. The second possible cycle uncovered in the present study involves tautomerization of **10** to form complex **13**, followed by reaction with alkyne *via* structure **14**. Release of the same product **4** from complex **15** completes the cycle and regenerates catalytically active nickel species.

In the present study we addressed the mechanism of alkyne insertion into the metal-phosphorus bond, since this pathway is most often discussed in the literature.[12,16,18] However, it should be pointed out that insertion of the alkyne into the metal-hydrogen bond is also a possible option,[17b] which requires further attention and more detailed elaboration.

Conclusions

We have developed the first acid-free, Ni-catalyzed synthetic procedure for the selective hydrophosphorylation of C≡C bonds. Addition of H-phosphonates to internal alkynes was performed with excellent stereoselectivity, and the addition reaction involving terminal alkynes was highly regioselective. Cheap and easily available $Ni(acac)_2$ salt was utilized as catalyst precursor. Markovnikov-type vinyl phosphonates were prepared in high yields using the developed catalytic system and isolated as pure products.

The strong ligand effect and catalyst precursor effect observed in the studied reaction arose from several specific requirements both on the catalyst activation step and the catalytic cycle itself. A detailed mechanistic study unveiled the nature of chemical transformations on the catalyst activation step. Formation of stable unreactive NiX_2L_n complexes, solubility and *in situ* reduction by the phosphine ligand are the key factors responsible for selection of the catalyst precursor. $Ni(acac)_2$ was found to be superior to fulfill the above criteria among the studied nickel salts.

The present study for the first time pointed out the importance of the tautomerization of pentavalent and trivalent phosphorus directly in the coordination sphere of the metal complex. The reaction pathway dealing with the Ni(II)–O–P(III) tautomeric form was discovered by theoretical calculations and the unique role of a bidentate ligand to control alkyne insertion step was highlighted. Undoubtedly, the further studies should be anticipated to get more insight into the mechanistic picture of these transformations and their possible application in carbon-phosphorus bond formation.

Experimental Section

General Description

All manipulations with $Ni(COD)_2$ were carried out in a glovebox under an argon atmosphere. In all other cases reaction vessels were argon flushed before heating. [$Ni(acac)_2$] was dried under vacuum (0.1–0.05 Torr, 60 °C, 0.5 h) before use. Other reagents were obtained from Acros and Aldrich and used as supplied (checked by NMR spectroscopy before use). THF was purified by distillation over the Na/benzophenone system, maintaining the intense blue color of benzophenone ketyl. Other solvents were purified according to

published methods. Unless otherwise noted, the reactions were carried out in PTFE screw capped tubes, equipped with a magnetic stirrer bar.

All NMR measurements were performed by using a three-channel Bruker AVANCE 500 spectrometer operating at 500.1, 202.5 and 125.8 MHz for ^{1}H, ^{31}P and ^{13}C nuclei, respectively. The spectra were processed on a Linux workstation by using TOPSPIN software package. The ^{1}H chemical shifts are reported relative to external TMS. The ^{13}C chemical shifts are reported relative to the corresponding solvent signals used as internal reference. The ^{31}P chemical shifts are reported relative to external H_3PO_4/H_2O.

Evaluation of the Ligand Effect (Table 1)

$[Ni(acac)_2]$ (3.0×10^{-5} mol, 7.7 mg), the ligand (6.0×10^{-5} mol for bidentate, 1.2×10^{-4} mol for monodentate) and THF (0.5 mL) were placed into the reaction vessel and stirred at room temperature for 5 min. **2a** (1.0×10^{-3} mol, 166.6×10^{-3} mL) and **1a** (1.0×10^{-3} mol, 131.7×10^{-3} mL) were added to the mixture and the reaction was carried out at 100 °C for 3 h under stirring.

Evaluation of Activity of Different Metal Precursors (Table 2)

The Ni compound (see Table 2 for details) used as metal precursor (6.0×10^{-5} mol), DPPE (12.0×10^{-5} mol, 47.8 mg) and THF (0.5 mL) were placed into the reaction vessel and stirred at room temperature for 5 min. **2a** (1.0×10^{-3} mol, 166.6×10^{-3} mL) and **1a** (1.0×10^{-3} mol, 131.7×10^{-3} mL) were added to the obtained mixture and the reaction was carried out at 100 °C for 6 h under stirring.

Analysis of the Influence of Additives (Table 3)

$[Ni(acac)_2]$ (6.0×10^{-5} mol, 15.4 mg), DPPE (12.0×10^{-5} mol, 47.8 mg) and THF (0.5 mL) were placed into the reaction vessel and stirred at room temperature for 5 min until a heterogeneous dark brown solution was formed (white precipitate was observed). **2a** (1.0×10^{-3} mol, 166.6×10^{-3} mL), **1a** (1.0×10^{-3} mol, 131.7×10^{-3} mL) and additive (see Table 3 for details) were transferred to the reaction vessel and the reaction was carried out at 100 °C for 24 h under stirring.

General Synthetic Procedure (Table 4), Purification and Characterization of Products

$[Ni(acac)_2]$ (9.0×10^{-5} mol, 23.1 mg), DPPE (18.0×10^{-5} mol, 71.7 mg) and THF (1.0 mL) were placed into the reaction vessel and stirred at room temperature for 5 min until a heterogeneous dark brown solution was formed (formation of a white precipitate was also observed). H-phosphonate **2** (1.0×10^{-3} mol), alkyne **1** (1.0×10^{-3} mol) were added to the obtained solution and the reaction was carried out at 100 °C (**1a–c**), 140 °C (**1d**), 120 °C (**1e**) for 24 h (**1a–c**), 30 h (**1d**), 20 h (**1e**) under stirring. Alkynes **1a–c** were added slowly using syringe pump (or by small portions manually) during 6 h from heating start.

After completion of the reaction the products were purified by dry column flash chromatography on silica. A hexanes/ethyl acetate gradient elution was applied. Dry column flash chromatography has several practical advantages: 1) only a small amount of silica required, 2) quick elution, and 3) economy of solvents. However, slightly better isolated yields (by ≈5–10%) may be achieved using conventional column chromatography.

After drying in vacuum the pure products were obtained. The isolated yields were calculated based on the initial amount of H-phosphonate **2**.

Diisopropyl (1-pentylvinyl)phosphonate (3a): ^{1}H NMR (500 MHz, $CDCl_3$): $\delta=0.90$ (t, $J_{H,H}=6.78$ Hz, 3H), 1.27–1.36 (m, 16H), 1.54 (m, 2H), 2.23 (m, 2H), 4.67 (m, 2H), 5.68 (d, $J_{P,H}=49.10$ Hz, 1H), 6.01 (d, $J_{P,H}=23.20$ Hz, 1H); $^{13}C\{^{1}H\}$ NMR (126 MHz, $CDCl_3$): $\delta=13.90$, 22.40, 23.78, 23.81, 24.02, 24.05, 27.40, 27.50, 31.30, 31.80, 31.90, 70.10, 70.20, 127.80 ($J_{P,C}=9.57$ Hz), 140.80 ($J_{P,C}=172.40$ Hz); $^{31}P\{^{1}H\}$ NMR (202 MHz, $CDCl_3$): $\delta=18.40$; MS (EI): *m/e* (%) = 262 (4) [M^+]; elemental analysis calcd. (%) for $C_{13}H_{27}O_3P$: C 59.52, H 10.37, P 11.81; found: C 59.63, H 10.31, P 11.84; yield: 0.166 g (63%).

Diisopropyl [1-(3-cyanopropyl)vinyl]phosphonate (3b): ^{1}H NMR (300 MHz, $CDCl_3$): $\delta=1.31$ (d, $J_{H,H}=6.20$ Hz, 6H), 1.35 (d, $J_{H,H}=6.20$ Hz, 6H), 1.93 (m, 2H), 2.34–2.50 (m, 4H), 4.70 (m, 2H), 5.77 (d, $J_{P,H}=47.90$ Hz, 1H), 6.09 (d, $J_{P,H}=22.60$ Hz, 1H); $^{13}C\{^{1}H\}$ NMR (75 MHz, $CDCl_3$): $\delta=$ 16.30, 23.70, 23.82, 23.85, 23.93, 23.98, 31.30, 31.40, 70.60, 70.70, 119.20, 129.80 ($J_{P,C}=9.61$ Hz), 138.70 ($J_{P,C}=$ 175.50 Hz); $^{31}P\{^{1}H\}$ NMR (121 MHz, $CDCl_3$): $\delta=16.50$; MS (EI): *m/e* (%) = 218 (77) [M^+-CH_3CN]; elemental analysis calcd. (%) for $C_{12}H_{22}NO_3P$: C 55.59, H 8.55, N 5.40, P 11.95; found: C 55.72, H 8.51, N 5.86, P 11.63; yield: 0.137 g (53%).

Diisopropyl (1-phenylvinyl)phosphonate (3c): ^{1}H NMR (500 MHz, $CDCl_3$): $\delta=1.20$ (d, $J_{H,H}=6.20$ Hz, 6H), 1.33 (d, $J_{H,H}=6.20$ Hz, 6H), 4.70 (m, 2H), 6.13 (d, $J_{P,H}=45.53$ Hz, 1H), 6.34 (d, $J_{P,H}=22.0$ Hz, 1H), 7.30–7.36 (m, 3H), 7.53–7.56 (m, 2H); $^{13}C\{^{1}H\}$ NMR (126 MHz, $CDCl_3$): $\delta=23.72$, 23.75, 24.14, 71.0, 71.05, 127.64, 127.68, 128.15, 128.35, 131.09, 137.15 ($J_{P,C}=11.41$ Hz), 141.25 ($J_{P,C}=175.45$ Hz); $^{31}P\{^{1}H\}$ NMR (202 MHz, $CDCl_3$): $\delta=15.45$; HR-MS (ESI): $m/z=286.1574$, calcd. for $[M+NH_4]^+$: 286.1567 ($\Delta=$ 2.40 ppm); elemental analysis calcd. (%) for $C_{14}H_{21}O_3P$: C 62.67, H 7.89, P 11.54; found: C 62.59, H 8.16, P 11.24; yield: 0.217 g (81%).

Diisopropyl [(1*E*)-1-ethylbut-1-en-1-yl]phosphonate (4a): ^{1}H NMR (500 MHz, $CDCl_3$): $\delta=1.05$ (m, 6H), 1.28 (d, $J_{H,H}=6.20$ Hz, 6H), 1.33 (d, $J_{H,H}=6.20$ Hz, 6H), 2.15–2.29 (m, 4H), 4.65 (m, 2H), 6.51 (dt, $J_{H,H}=7.30$ Hz, $J_{P,H\ cis}=$ 23.80 Hz, 1H); $^{13}C\{^{1}H\}$ NMR (126 MHz, $CDCl_3$): $\delta=13.10$, 13.90, 20.40, 20.50, 21.40, 21.50, 23.70, 23.80, 23.90, 24.00, 69.70, 69.71, 69.74, 69.80, 131.60 ($J_{P,C}=178.10$ Hz), 147.00 ($J_{P,C}=10.30$ Hz); $^{31}P\{^{1}H\}$ NMR (202 MHz, $CDCl_3$): $\delta=20.60$; MS (EI): *m/e* (%) = 248 (6) [M^+]; elemental analysis calcd. (%) for $C_{12}H_{25}O_3P$: C 58.05, H 10.15, P 12.47; found: C 58.29, H 9.83, P 12.49; yield: 0.171 g (69%).

Diisopropyl [(*E*)-1,2-diphenylvinyl]phosphonate (4b): ^{1}H NMR (500 MHz, $CDCl_3$): $\delta=1.23$ (d, $J_{H,H}=6.23$ Hz, 6H), 1.30 (d, $J_{H,H}=6.23$ Hz, 6H), 4.70 (m, 2H), 7.04–7.08 (m, 2H), 7.11–7.19 (m, 3H), 7.27–7.35 (m, 5H), 7.62 (d, $J_{P,H\ cis}=24.56$ Hz, 1H); $^{13}C\{^{1}H\}$ NMR (126 MHz, $CDCl_3$): $\delta=$ 23.86, 23.89, 24.10, 70.89, 70.93, 127.70, 128.20, 128.60, 128.80, 129.52, 129.55, 130.32, 132.77 ($J_{P,C}=180.74$ Hz), 135.00, 135.15, 135.91, 135.97, 142.70 ($J_{P,C}=10.79$ Hz); $^{31}P\{^{1}H\}$ NMR (202 MHz, $CDCl_3$): $\delta=16.43$; HR-MS (ESI):

m/z = 367.1438, calcd. for $[M+Na]^+$: 367.1434 (Δ = 1.10 ppm); elemental analysis calcd. (%) for $C_{20}H_{25}O_3P$: C 69.75, H 7.32, P 8.99; found: C 69.54, H 7.54, P 8.98; yield: 0.324 g (94%).

Diphenyl [(*E*)-1,2-diphenylvinyl]phosphonate (4c): ^{1}H NMR (500 MHz, $CDCl_3$): δ = 7.06–7.41 (m, 20H), 7.87 (d, $J_{P,H\ cis}$ = 26.21 Hz, 1H); $^{13}C\{^1H\}$ NMR (126 MHz, $CDCl_3$): δ = 120.57, 120.60, 125.05, 128.35, 128.42, 129.10, 129.68, 129.76, 130.70, 134.27, 134.46, 134.97, 146.45 ($J_{P,C}$ = 12.39 Hz), 150.63, 150.69; $^{31}P\{^1H\}$ NMR (202 MHz, $CDCl_3$): δ = 11.39; HR-MS (ESI): *m/z* = 435.1117, calcd. for $[M+Na]^+$: 435.1121 (Δ = 0.90 ppm); elemental analysis calcd. (%) for $C_{26}H_{21}O_3P$: C 75.72, H 5.13, P 7.51; found: C 75.65, H 5.15, P 7.48; yield: 0.367 g (89%).

Dibenzyl [(*E*)-1,2-diphenylvinyl]phosphonate (4d): ^{1}H NMR (500 MHz, $CDCl_3$): δ = 5.05 (d, $J_{P,H}$ = 7.69 Hz ,4H), 7.0–7.33 (m, 20H), 7.65 (d, $J_{P,H\ cis}$ = 25.05 Hz, 1H); $^{13}C\{^1H\}$ NMR (126 MHz, $CDCl_3$): δ = 67.69, 67.74, 127.87, 127.94, 128.26, 128.29, 128.52, 128.91, 129.15, 129.43, 129.47, 130.44, 130.88 ($J_{P,C}$ = 179.25 Hz), 134.59, 134.77, 135.34, 135.40, 136.35, 136.40, 144.06 ($J_{P,C}$ = 11.58 Hz); $^{31}P\{^1H\}$ NMR (202 MHz, $CDCl_3$): δ = 19.35; HR-MS (ESI): *m/z* = 441.1611, calcd. for $[M+H]^+$: 441.1614 (Δ = 0.70 ppm); elemental analysis calcd. (%) for $C_{28}H_{25}O_3P$: C 76.35, H 5.72, P 7.03; found: C 76.31, H 5.88, P 7.21; yield: 0.423 g (96%).

2-[(*E*)-1,2-Diphenylvinyl]-4,5-dimethyl-1,3,2-dioxaphospholane 2-oxide (4e): ^{1}H NMR (500 MHz, $CDCl_3$): δ = 0.96 (d, $J_{H,H}$ = 6.05 Hz, 3H), 1.28 (d, $J_{H,H}$ = 6.13 Hz, 3H), 3.22 (m, 1H), 4.21 (m, 1H), 7.04–7.46 (m, 10H), 7.81 (d, $J_{P,H\ cis}$ = 25.85 Hz, 1H); $^{13}C\{^1H\}$ NMR (126 MHz, $CDCl_3$): δ = 17.21, 17.29, 17.89, 17.94, 80.06, 83.24, 128.23, 128.31, 129.04, 129.51, 129.84, 129.88, 130.48, 134.36, 134.55, 135.07, 135.14, 146.61 ($J_{P,C}$ = 11.81 Hz); $^{31}P\{^1H\}$ NMR (202 MHz, $CDCl_3$): δ = 33.11; HR-MS (ESI): *m/z* = 337.0964, calcd. for $[M+Na]^+$: 337.0964 (Δ = 0 ppm); elemental analysis calcd. (%) for $C_{18}H_{19}O_3P$: C 68.78, H 6.09, P 9.85; found: C 68.44, H 6.23, P 9.82; yield: 0.308 g (98%).

Didodecyl [(*E*)-1,2-diphenylvinyl]phosphonate (4f): ^{1}H NMR (500 MHz, $CDCl_3$): δ = 0.88 (t, 6H), 1.20–1.33 (m, 36H), 1.57–1.65 (m, 4H), 3.97–4.07 (m, 4H), 7.03–7.37 (m, 10H), 7.62 (d, $J_{P,H\ cis}$ = 24.54 Hz, 1H); $^{13}C\{^1H\}$ NMR (126 MHz; $CDCl_3$): δ = 14.16, 22.75, 25.58, 29.22, 29.42, 29.62, 29.72, 30.50, 30.55, 31.99, 66.19, 66.24, 127.79, 128.21, 128.80, 128.95, 129.31, 130.39, 131.34 ($J_{P,C}$ = 179.97 Hz), 134.77, 134.95, 135.86, 143.52 ($J_{P,C}$ = 10.64 Hz); $^{31}P\{^1H\}$ NMR (202 MHz, $CDCl_3$): δ = 18.61; HR-MS (ESI): *m/z* = 619.4226, calcd. for $[M+Na]^+$: 619.4251 (Δ = 4.00 ppm); elemental analysis calcd. (%) for $C_{38}H_{61}O_3P$: C 76.47, H 10.30, P 5.19; found: C 76.51, H 10.20, P 5.21; yield: 0.585 g (98%).

Mechanistic Study of Catalyst Activation (Table 5).

DPPE (12.0×10^{-5} mol, 47.8 mg), **2a** (1.0×10^{-3} mol, 166.6×10^{-3} mL) and degassed THF-d_8 (0.5 mL) were transferred to an NMR tube. The Ni-containing (see Table 5 for details) metal precursor (6.0×10^{-5} mol) was added to obtained a colorless homogeneous solution, and the mixture was heated to 50 °C for 5 min and shaken. The ^{1}H and ^{31}P NMR spectra were recorded directly for the mixture (sample centrifugation was necessary in some cases to get better quality spectra).

All precipitates were isolated by centrifugation and dried under vacuum. Compounds $[NiCl_2(DPPE)]$, $[Ni(ClO_4)_2(DPPE)]$, $[Ni(ClO_4)_2(DPPE)_2]$ and $Ni(OAc)_2$ were washed thrice with 2 mL of degassed THF, the dioxide of DPPE was washed thrice with 2 mL of degassed hexane.

X-Ray Structural Study of 4e

Isolated product **4e** was dissolved in 2 mL of THF. Yellowish crystals were obtained after slow evaporation of the solvent at room temperature for a few days.

Single crystal X-ray diffraction experiments were carried out with a Bruker APEX2 1000 CCD area detector at 120 K using graphite monochromated Mo-Kα radiation (λ = 0.71073 Å). Experimental data have been corrected for absorption effects with the SADABS program.[34]

The structures were solved by direct methods and refined by the full-matrix least-squares against F^2 in anisotropic (for non-hydrogen atoms) approximation. All hydrogen atoms were placed in geometrically calculated positions and refined in isotropic approximation in a riding model. All calculations were performed using the SHELXTL software.[35]

Crystallographic data, refinement parameters and geometric parameters are provided in the Supporting Information, the molecular structure is shown on Figure 1. Crystallographic data for the structure reported in this study have been deposited with the Cambridge Crystallographic Data Centre under CCDC 784455. These data can be obtained free of charge from The Cambridge Crystallographic Data Centre *via* www.ccdc.cam.ac.uk/data_request/cif.

Theoretical Calculations

Geometry and energy of the reactants, intermediates, transition states and products of the reactions were calculated using the B3LYP hybrid density functional method[36] in conjunction with the standard 6-31G(d) basis set[37] for H, C, P, O and Lanl2dz basis set with effective core potentials[38] for the metal [denoted as B3LYP/DZ(d) level]. In previous studies it was established that this level of theory reasonably describes the energy and geometry parameters of the systems involving transition metal complexes.[39]

For all studied structures normal coordinate analysis was performed to characterize the nature of the stationary points and to calculate thermodynamic properties (298.15 K and 1 atm). Transition states were confirmed with IRC (intrinsic reaction coordinate) calculations using the standard method.[40] All calculations were performed without any symmetry constraints using the Gaussian 03 program.[41]

Acknowledgements

The research was supported in part by the Russian Foundation for Basic Research (Project No. 07-03-00851), Program No 1 of Division of Chemistry and Material Sciences of RAS and Program No 20 of RAS.

References

[1] a) *Green Chemistry: Theory and Practice*, (Eds.: P. T. Anastas, J. C. Warner), Oxford University Press, Oxford, **2000**; b) R. A. Sheldon, *Chem. Ind.* **1992**, 903.

[2] a) A. Togni, H. Grützmacher, (Eds), *Catalytic Heterofunctionalization*, Wiley-VCH, Weinheim, **2001**; b) F. Alonso, I. P. Beletskaya, M. Yus, *Chem. Rev.* **2004**, *104*, 3079; c) M. Beller, J. Seayad, A. Tillack, H. Jiao, *Angew. Chem.* **2004**, *112*, 3448; *Angew. Chem. Int. Ed.* **2004**, *43*, 3368; d) M. Suginome, Y. Ito, *J. Organomet. Chem.* **2003**, *685*, 218; e) M. Suginome, Y. Ito, *J. Organomet. Chem.* **2003**, *680*, 43; f) T. Kondo, T. Mitsudo, *Chem. Rev.* **2000**, *100*, 3205.

[3] Selected representative examples: a) A. Dzudza, T. Marks, *Chem. Eur. J.* **2010**, *16*, 3403; b) M. S. Hadfield, A. Lee, *Org. Lett.* **2010**, *12*, 484; c) T. Hirai, A. Hamasaki, A. Nakamura, M. Tokunaga, *Org. Lett.* **2009**, *11*, 5510; d) C. Liu, C. F. Bender, X. Han, R. A. Widenhoefer, *Chem. Commun.* **2007**, 3607; e) Y. Zhang, M. S. Sigman, *Org. Lett.* **2006**, *8*, 5557; f) C. Bruneau, P. H. Dixneuf, *Angew. Chem.* **2006**, *118*, 2232; *Angew. Chem. Int. Ed.* **2006**, *45*, 2176; g) N. T. Patil, L. M. Lutete, H. Wu, N. K. Pahadi, I. D. Gridnev, Y. Yamamoto, *J. Org. Chem.* **2006**, *71*, 4270; h) A. Kondoh, H. Yorimitsu, K. Oshima, *Org. Lett.* **2007**, *9*, 1383; i) D. A. Malyshev, N. M. Scott, N. Marion, E. D. Stevens, V. P. Ananikov, I. P. Beletskaya, S. P. Nolan, *Organometallics* **2006**, *25*, 4462; j) V. P. Ananikov, D. Malyshev, I. Beletskaya, G. Aleksandrov, I. Eremenko, *Adv. Synth. Catal.* **2005**, *347*, 1993; k) S. Burling, L. D. Field, B. A. Messerle, K. Q. Vuong, P. Turner, *Dalton Trans.* **2003**, 4181; l) A. Ogawa, *J. Organomet. Chem.* **2000**, *611*, 463; m) K. Alex, A. Tillack, N. Schwarz, M. Beller, *ChemSusChem* **2008**, *1*, 333; n) S. Hong, T. J. Marks, *Acc. Chem. Res.* **2004**, *37*, 673; o) A. Tillack, V. Khedkar, M. Beller, *Tetrahedron Lett.* **2004**, *45*, 8875; p) J. Hartwig, *Pure Appl. Chem.* **2004**, *76*, 507; q) F. Pohlki, S. Doye, *Chem. Soc. Rev.* **2003**, *32*, 104; r) L. Fadini, A. Togni, *Chem. Commun.* **2003**, 30; s) L. Ackermann, R. G. Bergman, *Org. Lett.* **2002**, *4*, 1475.

[4] Selected examples: a) C. Defieber, H. Grützmacher, E. M. Carreira, *Angew. Chem.* **2008**, *120*, 4558; *Angew. Chem. Int. Ed.* **2008**, *47*, 4482; b) C. Laporte, C. Böhler, H. Schönberg, H. Grützmacher, *J. Organomet. Chem.* **2002**, *641*, 227; c) W. Shi, Y. Luo, X. Luo, L. Chao, H. Zhang, J. Wang, A. Lei, *J. Am. Chem. Soc.* **2008**, *130*, 14713; d) P. Maire, S. Deblon, F. Breher, J. Geier, C. Böhler, H. Rüegger, H. Schönberg, H. Grützmacher, *Chem. Eur. J.* **2004**, *10*, 4198; e) R. Shintani, W.-L. Duan, K. Okamoto, T. Hayashi, *Tetrahedron: Asymmetry* **2005**, *16*, 3400.

[5] Selected examples: a) A. A. A. A. Quntar, R. Gallily, G. Katzavian, M. Srebnik, *Eur. J. Pharmacol.* **2007**, *556*, 9; b) Z. A. Doddridge, R. D. Bertram, C. J. Hayes, P. Soultanas, *Biochemistry* **2003**, *42*, 3239; c) K.-Y. Jung, R. J. Hohl, A. J. Wiemer, D. F. Wiemer, *Bioorg. Med. Chem.* **2000**, *8*, 2501; d) D. M. Cermak, D. F. Wiemer, K. Lewis, R. J. Hohl, *Bioorg. Med. Chem.* **2000**, *8*, 2729; e) L. Amori, G. Costantino, M. Marinozzi, R. Pellicciari, F. Gasparini, P. J. Flor, R. Kuhn, I. Vranesic, *Bioorg. Med. Chem. Lett.* **2000**, *10*, 1447; f) C. Vidil, A. Morere, M. Garcia, V. Barragan, B. Hamdaoui, H. Rochefort, J.-L. Montero, *Eur. J. Org. Chem.* **1999**, 447; g) W. Tian, Z. Zhu, Q. Liao, Y. Wu, *Bioorg. Med. Chem. Lett.* **1998**, *8*, 1949; h) P. S. Dragovich, S. E. Webber, R. E. Babine, S. A. Fuhrman, A. K. Patick, D. A. Matthews, C. A. Lee, S. H. Reich, T. J. Prins, J. T. Marakovits, E. S. Littlefield, R. Zhou, J. Tikhe, C. E. Ford, M. B. Wallace, J. W. Meador, R. A. Ferre, E. L. Brown, S. L. Binford, J. E. V. Harr, D. M. DeLisle, S. T. Worland, *J. Med. Chem.* **1998**, *41*, 2806; i) H. B. Lazrek, H. Khaïder, A. Rochdi, J.-L. Barascut, J.-L. Imbach, *Tetrahedron Lett.* **1996**, *37*, 4701.

[6] Representative examples of asymmetric synthesis of biologically active and related compounds: a) D.-Y. Wang, X.-P. Hu, J.-D. Huang, J. Deng, S.-B. Yu, Z.-C. Duan, X.-F. Xu, Z. Zheng, *Angew. Chem.* **2007**, *119*, 7956; *Angew. Chem. Int. Ed.* **2007**, *46*, 7810; b) T. Hayashi, T. Senda, Y. Takaya, M. Ogasawara, *J. Am. Chem. Soc.* **1999**, *121*, 11591; c) C. Giordano, G. Castaldi, *J. Org. Chem.* **1989**, *54*, 1470; d) A. A. Thomas, K. B. Sharpless, *J. Org. Chem.* **1999**, *64*, 8379; e) M. J. Burk, T. A. Stammers, J. A. Straub, *Org. Lett.* **1999**, *1*, 387; f) S. Sulzer-Mossé, M. Tissot, A. Alexakis, *Org. Lett.* **2007**, *9*, 3749; g) T. Yokomatsu, Y. Yoshida, K. Suemune, T. Yamagishi, S. Shibuya, *Tetrahedron: Asymmetry* **1995**, *6*, 365; h) G. Cravotto, G. B. Giovenzana, R. Pagliarin, G. Palmisano, M. Sisti, *Tetrahedron: Asymmetry* **1998**, *9*, 745; i) S. Vieth, B. Costisella, M. Schneider, *Tetrahedron* **1997**, *53*, 9623; j) J.-C. Henry, D. Lavergne, V. Ratovelomanana-Vidal, J.-P. Genet, I. P. Beletskaya, T. M. Dolgina, *Tetrahedron Lett.* **1998**, *39*, 3473.

[7] a) K. Zmudzka, T. Johansson, M. Wojcik, M. Janicka, M. Nowak, J. Stawinski, B. Nawrot, *New J. Chem.* **2003**, *27*, 1698; b) S. Abbas, R. D. Bertram, C. J. Hayes, *Org. Lett.* **2001**, *3*, 3365; c) M. R. Harnden, A. Parkin, M. J. Parratt, R. M. Perkins, *J. Med. Chem.* **1993**, *36*, 1343; d) H. B. Lazrek, A. Rochdi, H. Khaider, J.-L. Barascut, J.-L. Imbach, J. Balzarini, M. Witvrouw, C. Pannecouque, E. De Clercq, *Tetrahedron* **1998**, *54*, 3807; e) K. L. Agarwal, F. Riftina, *Nucleic Acids Res.* **1979**, *6*, 3009.

[8] Reviews: a) T. Minami, J. Motoyoshiya, *Synthesis* **1992**, 333; b) V. M. Dembitsky, A. A. A. A. Quntar, A. Haj-Yehia, M. Srebnik, *MiniRev. Org. Chem.* **2005**, *2*, 91; c) S. Failla, P. Finocchiaro, G. A. Consiglio, *Heteroat. Chem.* **2000**, *11*, 493; d) M. Maffei, *Curr. Org. Synth.* **2004**, *1*, 355; e) Y. Nagaoka, *Yakugaku Zasshi* **2001**, *121*, 771.

[9] a) J. Parvole, P. Jannasch, *Macromolecules* **2008**, *41*, 3893; b) T. Sato, M. Hasegawa, M. Seno, T. Hirano, *J. Appl. Polym. Sci.* **2008**, *109*, 3746; c) M. Schmider, E. Müh, J. E. Klee, R. Mülhaupt, *Macromolecules* **2005**, *38*, 9548; d) O. Senhaji, J. J. Robin, M. Achchoubi, B. Boutevin, *Macromol. Chem. Phys.* **2004**, *205*, 1039; e) J. R. Ebdon, D. Price, B. J. Hunt, P. Joseph, F. Gao, G. J. Milnes, L. K. Cunliffe, *Polym. Degrad. Stab.* **2000**, *69*, 267; f) S. Jin, K. E. Gonsalves, *Macromolecules* **1998**, *31*, 1010; g) W. R. Hertler, *J. Polym. Sci. A: Polym. Chem.* **1991**, *29*, 869.

[10] a) T. Bock, H. Möhwald, R. Mülhaupt, *Macromol. Chem. Phys.* **2007**, *208*, 1324; b) T. Ogawa, N. Usuki, N. Ono, *J. Chem. Soc. Perkin Trans. 1* **1998**, 2953; c) S. M.

Zakeeruddin, M. K. Nazeeruddin, P. Pechy, F. P. Rotzinger, R. Humphry-Baker, K. Kalyanasundaram, M. Grätzel, V. Shklover, T. Haibach, *Inorg. Chem.* **1997**, *36*, 5937; d) K. D. Belfield, C. Chinna, K. J. Schafer, *Tetrahedron Lett.* **1997**, *38*, 6131.

[11] a) C. M. Welch, E. J. Gonzales, J. D. Guthrie, *J. Org. Chem.* **1961**, *26*, 3270; b) F. J. Welch, H. J. Paxton, *J. Polym. Sci., Part A: Gen. Pap.*, **1965**, *3*, 3427; c) F. J. Welch, H. J. Paxton, *J. Polym. Sci., Part A: Gen. Pap.*, **1965**, *3*, 3439; d) S. V. Levchik, E. D. Weil, *Polym. Int.* **2005**, *54*, 11.

[12] a) M. Tanaka, *Top. Curr. Chem.* **2004**, *232*, 25; b) L. Coudray, J.-L. Montchamp, *Eur. J. Org. Chem.* **2008**, 3601; c) I. P. Beletskaya, M. A. Kazankova, *Russ. J. Org. Chem.* **2002**, *38*, 1391.

[13] a) D. K. Wicht, I. V. Kourkine, B. M. Lew, J. M. Nthenge, D. S. Glueck, *J. Am. Chem. Soc.* **1997**, *119*, 5039; b) D. K. Wicht, I. V. Kourkine, I. Kovacik, D. S. Glueck, T. E. Concolino, G. P. A. Yap, C. D. Incarvito, A. L. Rheingold, *Organometallics* **1999**, *18*, 5381; c) M. R. Douglass, T. J. Marks, *J. Am. Chem. Soc.* **2000**, *122*, 1824; d) M. R. Douglass, Ch. L. Stern, T. J. Marks, *J. Am. Chem. Soc.* **2001**, *123*, 10221; e) D. Mimeau, O. Delacroix, A.-C. Gaumont, *Chem. Commun.* **2003**, 2928; f) A. D. Sadow, I. Haller, L. Fadini, A. Togni, *J. Am. Chem. Soc.* **2004**, *126*, 14704; g) A. D. Sadow, A. Togni, *J. Am. Chem. Soc.* **2005**, *127*, 17012; h) H. Ohmiya, H. Yorimitsu, K. Oshima, *Angew. Chem.* **2005**, *117*, 2420; *Angew. Chem. Int. Ed.* **2005**, *44*, 2368; i) B. Join, D. Mimeau, O. Delacroix, A.-C. Gaumont, *Chem. Commun.* **2006**, 3249; j) I. Kovacik, C. Scriban, D. S. Glueck, *Organometallics* **2006**, *25*, 536; k) C. Scriban, D. S. Glueck *J. Am. Chem. Soc.* **2006**, *128*, 2788; l) A. Kondoh, H. Yorimitsu, K. Oshima, *J. Am. Chem. Soc.* **2007**, *129*, 4099; m) N. F. Blank, J. R. Moncarz, T. J. Brunker, C. Scriban, B. J. Anderson, O. Amir, D. S. Glueck, L. N. Zakharov, J. A. Golen, C. D. Incarvito, A. L. Rheingold, *J. Am. Chem. Soc.* **2007**, *129*, 6847.

[14] a) T. Mizuta, C. Miyaji, T. Katayama, J. Ushio, K. Kubo, K. Miyoshi, *Organometallics* **2009**, *28*, 539; b) P. Ribière, K. Bravo-Altamirano, M. I. Antczak, J. D. Hawkins, J.-L. Montchamp, *J. Org. Chem.* **2005**, *70*, 4064; c) L.-B. Han, Y. Ono, H. Yazawa, *Org. Lett.* **2005**, *7*, 2909.

[15] D. S. Glueck, *Top. Organomet. Chem.* **2010**, *31*, 65.

[16] a) L.-B. Han, M. Tanaka, *J. Am. Chem. Soc.* **1996**, *118*, 1571; b) Ch.-Q. Zhao, L.-B. Han, M. Goto, M. Tanaka, *Angew. Chem.* **2001**, *113*, 1983; *Angew. Chem. Int. Ed.* **2001**, *40*, 1929; c) L. B. Han, C. Zhang, H. Yazawa, S. Shimada, *J. Am. Chem. Soc.* **2004**, *126*, 5080.

[17] a) V. P. Ananikov, L. L. Khemchyan, I. P. Beletskaya, *Synlett* **2009**, 2375; b) V. P. Ananikov, L. L. Khemchyan, I. P. Beletskaya, *Russ. J. Org. Chem.* **2010**, *46*, 1269.

[18] N. Dobashi, K. Fuse, T. Hoshino, J. Kanada, T. Kashiwabara, C. Kobata, S. K. Nune, M. Tanaka, *Tetrahedron Lett.* **2007**, *48*, 4669.

[19] A number of other unidentified by-products (in addition to those shown in the scheme) may be also formed in the reaction, see the NMR spectrum of crude product in the Supporting Information to ref.[17a] and discussion therein.

[20] In the literature selectivity was often defined as a simple ratio between Markovnikov and anti-Markovnikov products (Scheme 1), while the other by-products are neglected. Although such calculations gave higher selectivity values, catalyst optimization resulted in lower isolated yields due to formation of other by-products. Throughout the present study the material balance on phosphorus species was verified in each experiment (the product, unreacted H-phosphonate and overall amount of by-products).

[21] V. P. Ananikov, D. A. Malyshev, I. P. Beletskaya, *Adv. Synth. Catal.* **2005**, *347*, 1993.

[22] Nickel complexes are known to catalyze alkyne polymerization: a) P. W. Jolly, G. Wilke, *The Organic Chemistry of Nickel*, Academic Press, New York, **1974**; b) T. Masuda, F. Sanda, M. Shiotsuki, *Polymerization of Acetylenes*, in: *Comprehensive Organometallic Chemistry III*, (Eds.: D. M. P. Mingos, R. H. Crabtree), Vol. 11, Elsevier Ltd., Oxford, **2007**, pp 557–593; c) V. P. Ananikov, K. A. Gayduk, I. P. Beletskaya, V. N. Khrustalev, M. Yu. Antipin, *Chem. Eur. J.* **2008**, *14*, 2420.

[23] The contribution of the side reaction of alkyne polymerization was negligible in the case of internal alkynes, thus resulting in higher product yields (see ref.[22]).

[24] Observed [M−ClO_4] peaks in ESI-MS at 555.0192 and 953.1553 Da, calculated peaks: 555.0186 and 953.1540 Da, respectively. ^{31}P NMR (DMSO): $\delta = 56.3$, 30.4, 30.2, −13.9, −14.2.

[25] Formation of a broad signal is an indication of complexation to the metal center (or exchange), see: a) D. C. Roe, P. M. Kating, P. J. Krusic, B. E. Smart, *Top. Catal.* **1998**, *5*, 133; b) D. S. Glueck, *Coord. Chem. Rev.* **2008**, *252*, 2171; c) P. S. Pregosin, *Coord. Chem. Rev.* **2008**, *252*, 2156; d) P. S. Pregosin, (Ed.), *Transition Metal Nuclear Magnetic Resonance*, Elsevier, Amsterdam, **1991**.

[26] In the present study we did not investigate the influence of the metal salt on by-products formation, since in the optimized conditions high product yields were obtained.

[27] Reduction of Pd(II) in catalytic reactions (*in situ*): N. Clayden, N. Greeves, S. Warren, P. Wothers, *Organic Chemistry*, Oxford University Press, **2001**, p 1322.

[28] External nucleophilic attack is more common for π-complexes of divalent metal derivatives, although involvement of π-complexes of zero-valent metal derivatives can not be excluded. In the studied system Ni(II) and Ni(0) centers can be readily interconverted by oxidative addition/reductive elimination of the P−H bond (in Scheme 3 ligands on Ni are omitted for clarity).

[29] Alkyne insertion into the M−P bond was studied in detail, this insertion reaction was assumed as the key stage of reaction mechanism in a number of studies (see refs.[12,16,18]).

[30] Under the experimental conditions formation of complexes with X = H or phosphorus group were discussed (see refs.[12,16–18]), for the calculations here the simple model with X = H was utilized.

[31] a) J. Stawinski, A. Kraszewski, *Acc. Chem. Res.* **2002**, *35*, 952; b) J.-N. Li, L. Liu, Y. Fu, Q.-X. Guo, *Tetrahe-*

dron **2006**, *62*, 4453; c) J. P. Guthrie, *Can. J. Chem.* **1979**, *57*, 236.

[32] At the moment it is not possible to unambiguously rule out either of the pathways due to known limitations of calculation accuracy. See the reviews for a discussion of the accuracy of density functional calculations for studying reaction mechanisms of transition metal-catalyzed transformations: a) V. P. Ananikov, D. G. Musaev, K. Morokuma, *J. Mol. Cat. A: Chem.* **2010**, *324*, 104; b) C. J. Cramer, D. G. Truhlar, *Phys. Chem. Chem. Phys.* **2009**, *11*, 10757.

[33] A similar mechanism is applicable for the $Ni(COD)_2$ precursor, where NiL_n species are generated by ligand exchange reaction (see Scheme 3 and related discussion).

[34] G. M. Sheldrick, *SADABS*, **1997**, Bruker AXS Inc.,Madison, WI-53719, USA.

[35] G. M. Sheldrick, *SHELXTL-97*, Version 5.10, Bruker AXS Inc., Madison, WI-53719, USA.

[36] a) A. D. Becke, *Phys. Rev. A* **1988**, *38*, 3098; b) C. Lee, W. Yang, R. G. Parr, *Phys. Rev. B* **1988**, *37*, 785; c) A. D. Becke, *J. Chem. Phys.* **1993**, *98*, 5648.

[37] a) R. Ditchfield, W. J. Hehre, J. A. Pople, *J. Chem. Phys.* **1971**, *54*, 724; b) W. J. Hehre, R. Ditchfield, J. A. Pople, *J. Chem. Phys.* **1972**, *56*, 2257.

[38] a) P. J. Hay, W. R. Wadt, *J. Chem. Phys.* **1985**, *82*, 270; b) P. J. Hay, W. R. Wadt, *J. Chem. Phys.* **1985**, *82*, 284; c) P. J. Hay, W. R. Wadt, *J. Chem. Phys.* **1985**, *82*, 299; d) T. H. Dunning Jr, P. J. Hay, in: *Modern Theoretical Chemistry*, (Ed.: H. F. Schaefer III), Vol. 3, Plenum, New York, **1976**, pp 1–28.

[39] a) V. P. Ananikov, R. Szilagyi, D. G. Musaev, K. Morokuma, *Organometallics* **2005**, *24*, 1938; b) see also refs.[32a,b]

[40] a) C. Gonzalez, H. B. Schlegel, *J. Chem. Phys.* **1989**, *90*, 2154; b) C. Gonzalez, H. B. Schlegel, *J. Phys. Chem.* **1990**, *94*, 5523.

[41] M. J. Frisch and co-workers, *Gaussian 03*, Gaussian, Inc., Pittsburgh PA, **2003**.

